Optics Letters

Intra-cavity pumped Yb:YAG thin-disk laser with 1.74% quantum defect

CHRISTIAN VORHOLT* AND ULRICH WITTROCK

Photonics Laboratory, Muenster University of Applied Sciences, Stegerwaldstraße 39, 48565 Steinfurt, Germany
Corresponding author: cvorholt@fh-muenster.de

We present, to the best of our knowledge, the first intra-cavity pumped Yb:YAG thin-disk laser. It operates at 1050.7 nm with a quantum defect of just 1.74% due to pumping at 1032.4 nm. Low absorption of the pump light at the pump wavelength of 1032.4 nm is compensated for by placing the disk inside the resonator of another Yb:YAG thin-disk laser which is diode-pumped at 940 nm. The intra-cavity pumped laser has an output power of 10.3 W and a slope efficiency of 8.3%.   © 2015 Optical Society of America

Optically pumped lasers usually convert a pump beam of low brightness into a laser beam of higher brightness. The efficiency of these brightness converters is limited by the second law of thermodynamics which dictates that a certain fraction of the pump energy must be expelled to the environment if the brightness is increasing [1]. This fraction of the pump energy is called the quantum defect, and it is the energy difference of the pump photon and the laser photon. It is usually transferred to the environment as heat. The quantum defect is often the main source of heat in solid-state lasers. Heat generation leads to a nonuniform distribution of temperature inside the gain medium [2]. As a consequence, the beam quality of the laser is degraded by thermo-optical aberrations. Quasi-three level lasers such as Yb:YAG exhibit only a small quantum defect, but they have to be pumped hard to obtain efficient laser emission at room temperature. The availability of high brightness laser diodes for optical pumping at 940 nm and the invention of the thin-disk laser facilitated efficient laser emission of Yb:YAG [3].

The energy level diagram of Yb:YAG is shown in Fig. 1. The Yb^{3+}-ion has only two electronic states: the ground state $^2F_{7/2}$ and the excited state $^2F_{5/2}$. The Stark effect splits the ground state into four energy levels and the excited state into three levels. Yb:YAG thin-disk lasers are usually pumped at 940 nm and emit laser radiation around 1030 nm, exhibiting a quantum defect of 8.7%. Weichelt *et al.* presented a thin-disk laser that

was pumped at 969 nm; hence, the quantum defect was 5.9% [5]. Their laser was pumped from Z_1, the lowest energy level of the ground state, directly into the upper laser level A_1. Pumping from Z_1 facilitates high absorption at the pump wavelength because the energy level Z_1 is strongly populated, even at temperatures well above room temperature. When the laser is pumped from Z_1, the quantum defect cannot be made smaller than the energy difference between the energy levels Z_1 and Z_2. A further reduction of the quantum defect requires pumping from Z_2, Z_3, or Z_4. The lowest possible quantum defect in Yb:YAG can be achieved by pumping from Z_2 to A_1 and lasing from A_1 to Z_3. This laser would have a quantum defect of approximately 0.4%, but has not been shown yet.

Our intra-cavity pumped laser is pumped from the energy level Z_3 directly into the upper laser level A_1. Lasing occurs between A_1 and Z_4. White proposed level parameters to quantify the system level of lasers [6]. A level parameter of four indicates a four-level laser, and a level parameter of two would indicate an (impossible) two-level laser. According to these level parameters, the level parameter of our laser is 2.05 at room temperature. However, the quasi-two-level system comes at a price: Yb:YAG needs to be pumped hard to achieve gain at the weak
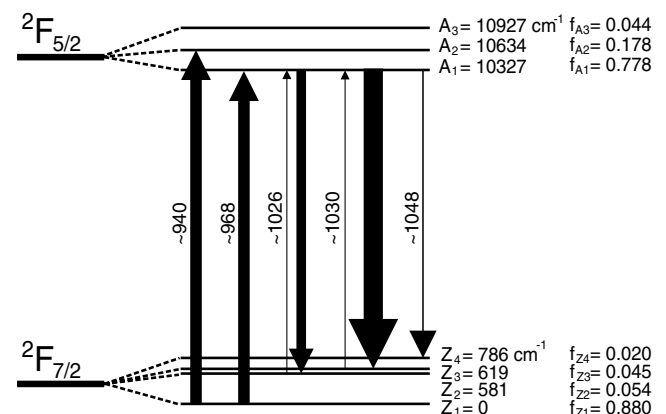
Fig. 1. Energy level diagram of Yb:YAG at 300 K [4]. The energies are denoted by Z in the lower multiplet and A in the upper multiplet; the relative occupation numbers at room temperature are denoted by f. The thicknesses of the arrows are proportional to the effective cross sections of the transitions.

$A_1 \rightarrow Z_4$ laser transition, and the absorption at the $Z_3 \rightarrow A_1$ pump transition is very low. The standard solution to compensate for the low absorption is the use of a multipass pumping scheme. Thin-disk lasers use multipass pumping schemes involving a parabolic mirror [7]. However, the number of pump passes is limited by the accessible solid angle and the beam quality of the pump [8]. We compensate for the low pump absorption at the $Z_3 \rightarrow A_1$ transition by placing the disk inside the resonator of another diode-pumped thin-disk laser. In other words, we use the resonant enhancement inside the resonator of the diode-pumped thin-disk laser to increase the absorption. When the second disk is pumped, but has not reached its lasing threshold, its $^2F_{7/2}$-manifold is depleted, and absorption for the pump radiation is reduced. If it is then pumped harder, and lasing occurs; the $^2F_{7/2}$-manifold is repopulated due to stimulated emission at the $A_1 \rightarrow Z_4$ laser transition. Hence, the intra-cavity power of the intra-cavity pumped laser has to be high to ensure repopulation of the $^2F_{7/2}$-manifold. This discussion shows that the two lasers are coupled, and a joint solution of their rate equations is required. The strong nonlinear coupling can result in chaotic laser emission, self-sustained pulsations, and continuous-wave laser emission. All of these have been observed in our experiments. The solutions of the coupled rate equations leading to chaotic laser emission and self-sustained pulsations will be discussed in a full-length paper [9].

The experimental setup is shown in Fig. 2. The resonator of the diode-pumped thin-disk laser is V-shaped and comprises a dichroic mirror and two identical disks. The disks have the same thickness d of 130 μm and doping concentration n_{dop} of 9 at. %. One disk sits at the vertex of the "V" and is pumped by diode lasers at 940 nm. A multipass pumping scheme consisting of a parabolic mirror and three prisms establishes 16 single passes through the diode-pumped disk. The intra-cavity pumped disk serves as the output coupler of the resonator by absorbing a small fraction of the intra-cavity power. The opposite end of the resonator is terminated by a dichroic mirror. This mirror has a reflectivity greater than 99.5% at 1030 nm and a reflectivity smaller than 45% at 1048 nm. Its purpose is to force the diode-pumped laser to operate around 1030 nm. Otherwise, the laser would operate around 1048 nm to avoid the loss due to absorption by the second disk. The intra-cavity pumped laser is set up with a V-resonator as well. The end mirrors of this V-resonator are two HR mirrors; both mirrors are
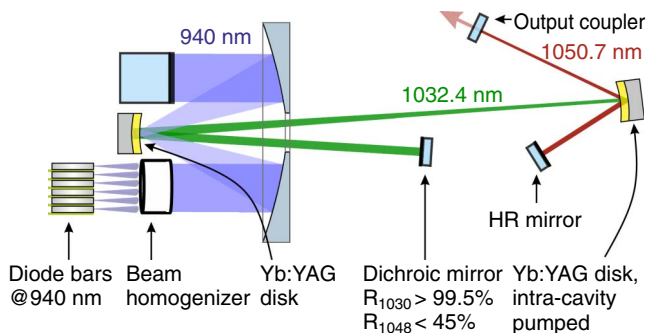
specified for having a reflectivity greater than 99.98%. Transmission measurements revealed a slightly higher transmission of one mirror; thus, this one effectively served as the output coupling mirror.

We now want to calculate the wavelength of the diode-pumped laser and compare it with the experiment. The wavelength is determined by the spectral gain, the linear spectral losses of the dichroic mirror, and the nonlinear spectral losses due to absorption in the intra-cavity pumped disk. Above threshold, the optimal output coupling of the intra-cavity pumped laser could be determined using the laser-pumped-laser model developed by Brown [10]. At the threshold of the intra-cavity pumped laser, the saturation of its pump transition is negligible, and we can replace the nonlinear losses by linear ones. This is the case we now want to study, and we defer the general case to the full-length paper. For the sake of simplicity, we assume that both disks have the same temperature. Intra-cavity losses due to scattering and impurity absorption are neglected because they are small compared to the small-signal loss of 3.6% per round-trip due to absorption by the second disk. The saturation intensity at the vacuum wavelength λ is given by $I_{sat}(\lambda) = hc_0/[\lambda(\sigma_{abs}(\lambda) + \sigma_{em}(\lambda))\tau_{10}]$, where τ_{10} is the upper state lifetime of Yb:YAG, h is Planck's constant, $\sigma_{abs}(\lambda)$ and $\sigma_{em}(\lambda)$ are the effective cross sections for absorption and emission at the wavelength λ, and c_0 is the speed of light in vacuum. In the following, all intensities are normalized to their saturation intensity, quantities referring to the diode-pumped disk are denoted by (d), and quantities referring to the intra-cavity pumped disk are denoted by (i). The gain-loss balance equation of the diode-pumped laser at the lasing threshold is given by

$$\underbrace{\exp[M_L^{(d)} g_0^{(d)}(\lambda) d]}_{\substack{\text{Round-trip gain} \\ \text{of the} \\ \text{diode-pumped disk}}} = \underbrace{1/(1 - T_{dic}(\lambda))}_{\substack{\text{Loss due to} \\ \text{transmission of the} \\ \text{dichroic mirror}}} \underbrace{\exp[M_P^{(i)} \alpha_0^{(i)}(\lambda) d]}_{\substack{\text{Round-trip transmission} \\ \text{of the intra-cavity} \\ \text{pumped disk}}}. \quad (1)$$

$M_L^{(d)} = 4$ is the number of amplification passes of the laser beam through the diode-pumped disk per round-trip, $g_0^{(d)}(\lambda)$ is the small-signal gain coefficient which will be derived below, d is the thickness of the disks, $T_{dic}(\lambda)$ is the spectral transmission of the dichroic mirror, $M_P^{(i)} = 2$ is the number of pump passes of the laser beam through the intra-cavity pumped disk per round-trip, and $\alpha_0^{(i)}(\lambda)$ is its small-signal absorption coefficient at the wavelength λ given by $\alpha_0^{(i)}(\lambda) = \sigma_{abs}^{(i)}(\lambda)n_{dop}$, where $\sigma_{abs}^{(i)}(\lambda)$ is the effective cross section for absorption. The multipass pumping scheme of the diode-pumped laser requires the introduction of an effective pump intensity $i_{P,eff}^{(d)}$. The effective pump intensity results from the 16 passes of the pump light through the diode-pumped disk [11]. Since the high pump intensity in thin-disk lasers leads to partial saturation of the pump transition, the effective pump intensity depends on the degree of saturation:

$$i_{P,eff}^{(d)}(\alpha_P^{(d)}) = i_{P,D}^{(d)} \frac{1 - \exp[-M_P^{(d)} \alpha_P^{(d)}(i_{P,eff}^{(d)})d]}{\alpha_P^{(d)}(i_{P,eff}^{(d)})d}, \quad (2)$$

where $i_{P,D}^{(d)}$ is the intensity of the pump diodes on the first pass of the pump beam through the disk, normalized to the saturation intensity at 940 nm; $M_P^{(d)} = 16$ is the number of pump passes through the diode-pumped disk; $\alpha_P^{(d)}$ is the saturated absorption coefficient of the disk given by $\alpha_P^{(d)}(i_{P,eff}^{(d)}) = \alpha_{P,0}^{(d)}/[1 + i_{P,eff}^{(d)}(\alpha_P^{(d)})]$; and $\alpha_{P,0}^{(d)}$ is the small-signal absorption coefficient of the diode-pumped disk for the 940 nm pump

Fig. 2. Experimental setup of the intra-cavity pumped thin-disk laser. At a diode pump power of 300 W, the diode-pumped laser oscillates at 1032.4 nm, and the intra-cavity pumped laser oscillates at 1050.7 nm.

light. When deriving Eq. (2), we assumed a single pass absorption that is much smaller than unity and assumed that the effective pump intensity is constant within the disk. Please note that Eq. (2) is an implicit equation because $i_{P,eff}^{(d)}$ is a function of $\alpha_P^{(d)}$ as expressed on the left side, but the right side contains $\alpha_P^{(d)}$ as a function of $i_{P,eff}^{(d)}$ in two instances. The small-signal gain coefficient $g_0^{(d)}(\lambda)$ that includes the reduced absorption due to the depletion of the $^2F_{7/2}$-manifold of the diode-pumped disk was derived in Eq. (14) of our previous publication [12],

$$g_0^{(d)}(\lambda) = \alpha_{L,0}^{(d)}(\lambda) \frac{(B^{(d)}(\lambda) - 1)i_{P,eff}^{(d)} - 1}{1 + i_{P,eff}^{(d)}}, \qquad (3)$$

where $\alpha_{L,0}^{(d)}(\lambda)$ is the small-signal absorption coefficient of the diode-pumped disk. $B^{(d)}$ is a ratio of the cross sections for the diode-pumped disk which we define as follows:

$$B^{(d)}(\lambda) := \frac{\sigma_{abs,940}^{(d)}[\sigma_{abs}^{(d)}(\lambda) + \sigma_{em}^{(d)}(\lambda)]}{\sigma_{abs}^{(d)}(\lambda)[\sigma_{abs,940}^{(d)} + \sigma_{em,940}^{(d)}]}. \qquad (4)$$

For our calculations, we use measured effective absorption and emission cross sections at 300 K from Koerner et al. [13]. Inserting Eq. (3) into Eq. (1), and solving for the effective pump intensity $i_{P,eff}^{(d)}$, yields the normalized effective pumped intensity at the lasing threshold $i_{P,eff,th}^{(d)}(\lambda)$ of the diode-pumped laser as a function of the wavelength

$$i_{P,eff,th}^{(d)}(\lambda) = \frac{B^{(d)}M_L^{(d)}\alpha_{L,0}^{(d)}(\lambda)d}{\ln[1 - T_{dic}(\lambda)] + \alpha_{L,0}^{(d)}(\lambda)d[M_L^{(d)}(B^{(d)} - 1) - M_P^{(i)}]} - 1. \qquad (5)$$

The diode pump intensity $i_{P,D,th}^{(d)}(\lambda)$ which is required for reaching the threshold of the diode-pumped laser can be calculated by inserting Eq. (5) into Eq. (2). Figure 3 shows this diode pump intensity $i_{P,D,th}^{(d)}(\lambda)$ as a function of wavelength. The observed mean laser wavelength of 1032.4 nm fits well to the calculated wavelength that requires the lowest effective pump power.
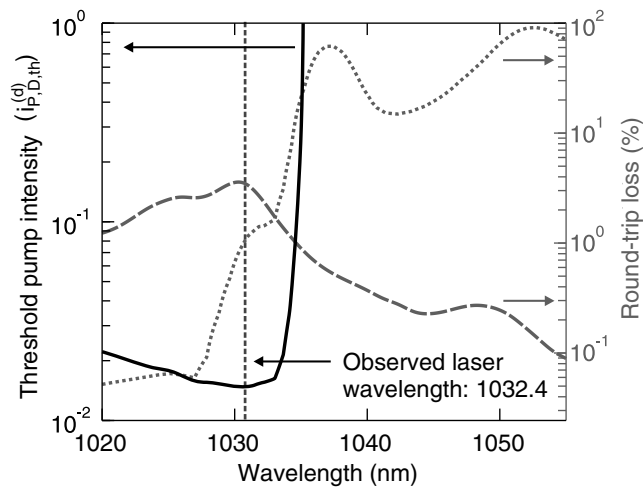
In the experiments, both disks were pumped with circular spots having flat-top intensity profiles to a good approximation. The spots on the diode-pumped disk and on the intra-cavity pumped disk initially had a diameter of 5.5 and 5.6 mm, respectively. With these spot diameters, continuous-wave laser output was achieved. When the pump spot on the intra-cavity pumped disk was made smaller than 1.5 mm, chaotic intensity fluctuations or self-sustained pulsations occurred, depending on the pump spot diameter. All subsequent measurements were carried out with a pump spot diameter of 5.6 mm on the intra-cavity pumped disk to avoid intensity fluctuations.

Figure 4 shows the measured optical spectra of the diode-pumped laser and the intra-cavity pumped laser in transverse multimode operation. The optical spectra were measured with an optical spectrum analyzer (HP 71450B), having a spectral resolution of 0.1 nm. When the intra-cavity pumped laser starts oscillating, both thin-disk lasers emit at two wavelengths each. Three wavelengths can be identified in the optical spectrum of the intra-cavity pumped thin-disk laser at high pumping powers. We have shown that spatial hole burning enables the simultaneous oscillation of several longitudinal modes with a frequency spacing many times larger than the free spectral range of the resonator [12]. At the maximum applied diode pump power of 300 W, the diode-pumped laser was oscillating at a weighted mean wavelength of 1032.4 nm, and the intra-cavity pumped laser was oscillating at a weighted mean wavelength of 1050.7 nm. Hence, the quantum defect was just 1.74%. Figure 5 shows the measured output power of the intra-cavity pumped laser and the power of the diode-pumped laser that leaked through the dichroic mirror. The diode-pumped laser has a threshold of 132 W which compares well with the value of 121 W for our mean pump wavelength of 934 nm. The maximum output power in transverse multimode operation of the intra-cavity pumped laser was 10.3 W at a diode pump power of 300 W; in addition, approximately 500 mW were transmitted by the HR mirror. At the same pumping power, 28 W from the diode-pumped laser leaked

Fig. 3. From 1030 to 1035 nm, the loss due to transmission of the dichroic mirror (dotted, gray) is increasing rapidly while the unsaturated absorption of the intra-cavity pumped disk (dashed, gray) is decreasing, leading to a minimum of the threshold pump intensity (solid, black) at 1032.4 nm where lasing will start.
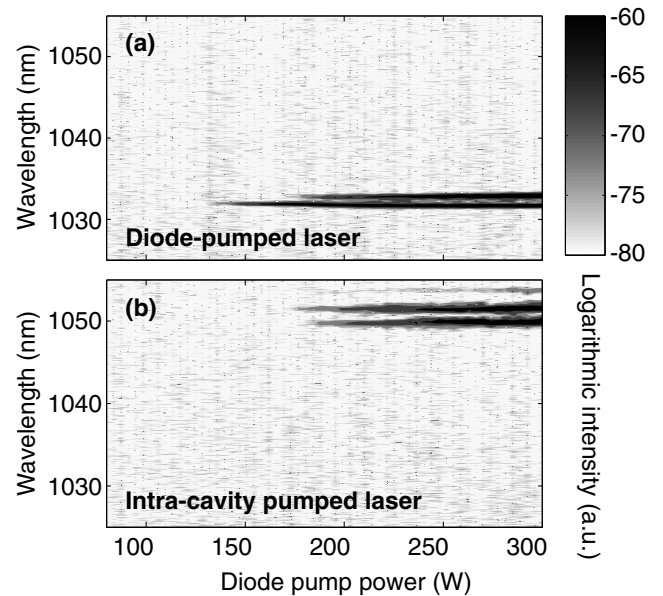
Fig. 4. (a) Measured optical spectrum of the diode-pumped laser and (b) measured optical spectrum of the intra-cavity pumped laser.
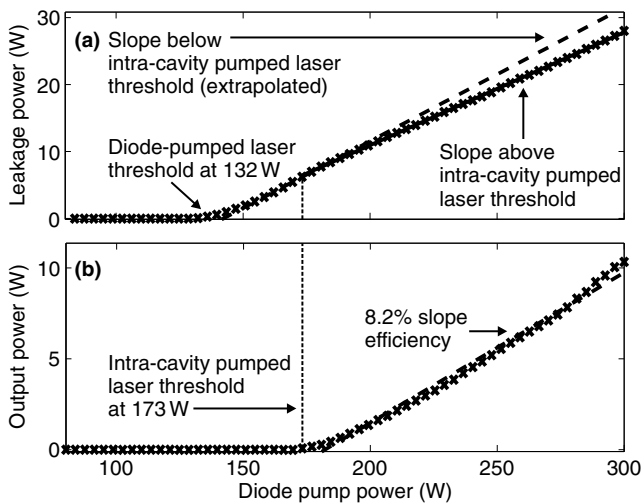
Fig. 5. (a) Measured leakage power transmitted through the dichroic mirror of the diode-pumped laser and (b) measured output power of the intra-cavity pumped laser in transverse multimode operation.

quantum defect of 1.74% minimizes thermo-optical aberrations in the gain medium if the laser can be scaled to high output power. The concept of intra-cavity pumping can also be used for optical cooling of solids having a small absorption at the pump wavelength. One example is the VECSEL laser demonstrated by Ghasemkhani *et al.* which was intra-cavity pumped by a diode laser [15].

Finally, the availability of spectral filters with a sharper spectral edge would increase the efficiency. Instead of using the combination of 1032.4 and 1050.7 nm for the pump laser and the intra-cavity pumped laser, one could also use the combination 1026 and 1030 nm. Yb:YAG has sufficiently high cross sections at these wavelengths and, with a quantum defect of just 0.4%, the laser would operate even closer to the thermodynamic limit. This, however, requires a spectral filter with an even sharper edge.

through its dichroic mirror. When the lasing threshold of the intra-cavity pumped laser is reached at 173 W of diode pump power, the slope of the output power of the diode-pumped laser decreases which indicates that the stimulated emission in the second disk repopulates its $^2F_{7/2}$-manifold and, therefore, increases the absorption of the second disk.

The experimental results show that the diode-pumped laser oscillates at a wavelength where the reflectivity of the dichroic mirror is only 99%, leading to substantial losses. The reflectivity of an ideal dichroic mirror would be 100% at 1030 nm and zero for longer wavelengths. A dielectric coating that comes close to such a step function is difficult to manufacture because it requires many precisely spaced dielectric layers. In principle, the spectral tuning element does not have to be a mirror; any other spectral filter could be used if it has low losses and can be operated with intra-cavity powers in the multi-kilowatt regime. Nevertheless, for high intra-cavity powers, mirrors as spectral filters seem to be more suitable than transmissive intra-cavity filters. Recently, Schuhmann and Larionov presented a thin-disk laser that was stabilized at a wavelength of 1030 nm by using an auxiliary cavity as end mirror; it comprises an output coupler and a volume Bragg grating [14]. The auxiliary cavity is suitable for high power application and has a spectral bandwidth that is determined by the volume Bragg grating. We have not tested the performance of such an auxiliary cavity for our intra-cavity pumped laser yet.

In conclusion, we have presented, to the best of our knowledge, the first intra-cavity pumped thin-disk laser. The low

REFERENCES

1. C. E. Mungan, J. Opt. Soc. Am. B **20**, 1075 (2003).
2. J. Perchermeier and U. Wittrock, Opt. Lett. **38**, 2422 (2013).
3. A. Giesen, H. Huegel, A. Voss, K. Wittig, U. Brauch, and H. Opower, Appl. Phys. B. **58**, 365 (1994).
4. A. Brenier, Y. Guyot, H. Canibano, G. Boulon, A. Ródenas, D. Jaque, A. Eganyan, and A. G. Petrosyan, J. Opt. Soc. Am. B **23**, 676 (2006).
5. B. Weichelt, A. Voss, M. Abdou Ahmed, and T. Graf, Opt. Lett. **37**, 3045 (2012).
6. J. O. White, IEEE J. Quantum Electron. **45**, 1213 (2009).
7. S. Erhard, A. Giesen, M. Karszewski, T. Rupp, C. Stewen, I. Johannsen, and K. Contag, in *Advanced Solid-State Lasers, OSA Trends in Optics and Photonics*, Boston, Mass., 1999, p. 38.
8. K. Albers and U. Wittrock, Appl. Phys. B **105**, 245 (2011).
9. C. Vorholt and U. Wittrock are preparing a manuscript to be called "Laser dynamics in intra-cavity pumped thin-disk lasers."
10. D. C. Brown, Laser Phys. **24**, 085002 (2014).
11. K. Contag, M. Karszewski, C. Stewen, A. Giesen, and H. Huegel, Quantum Electron. **29**, 697 (1999).
12. C. Vorholt and U. Wittrock, Appl. Phys. B **120**, 711 (2015).
13. J. Körner, C. Vorholt, H. Liebetrau, M. Kahle, D. Kloepfel, R. Seifert, J. Hein, and M. C. Kaluza, J. Opt. Soc. Am. B **29**, 2493 (2012).
14. K. Schuhmann and M. Larionov, *Advanced Solid-State Lasers Congress (ASSL)* (2013).
15. M. Ghasemkhani, A. Albrecht, S. Melgaard, D. Seletskiy, J. Cederberg, and M. Sheik-Bahae, *Conference on Lasers and Electro-Optics*, OSA Technical Digest (online) (Optical Society of America, 2013).